

New Mineral Names*†

FERNANDO CÁMARA¹, OLIVIER C. GAGNE², YULIA UVAROVA³ AND DMITRIY I. BELAKOVSKIY⁴

¹Dipartimento di Scienze della Terra, Università di degli Studi di Torino, Via Valperga Caluso, 35-10125 Torino, Italy

²Department of Geological Sciences, University of Manitoba, Winnipeg, Manitoba R3T 2N2, Canada

³CSIRO Mineral Resources, CSIRO, ARRC, 26 Dick Perry Avenue, Kensington, Western Australia 6151, Australia

⁴Fersman Mineralogical Museum, Russian Academy of Sciences, Leninskiy Prospekt 18 korp. 2, Moscow 119071, Russia

IN THIS ISSUE

This New Mineral Names has entries for 15 new minerals, including antipinite, anzaite-(Ce), bettertonite, bobshannonite, calcinaksite, khvorovite, leguernite, lukkulaisvaaraite, minjiangite, möhnite, moraskoite, nickelpicromerite, pilawite-(Ce), ralpcannonite, and yeomanite.

ANTIPINITE*

N.V. Chukanov, S.M. Aksenov, R.K. Rastsvetaeva, K.A. Lysenko, D.I. Belakovskiy, G. Färber, G. Möhn and K.V. Van (2015) Antipinite, $\text{KNa}_3\text{Cu}_2(\text{C}_2\text{O}_4)_4$, a new mineral species from a guano deposit at Pabellón de Pica, Chile. Mineralogical Magazine, 79(5), 1111–1121.

Antipinite (IMA 2014-027), ideally $\text{KNa}_3\text{Cu}_2(\text{C}_2\text{O}_4)_4$, was discovered in the guano deposit at the lower part of the northern slope of Pabellón de Pica Mountain, Tarapacá Region, Chile. The new mineral honors Mikhail Yuvenal'evich Antipin (1951–2013), a Russian specialist in the crystallography and crystal chemistry of organometallic and coordination compounds. Antipinite occurs in association with halite, salammoniac, chanabayaite, and joanneumite. The host gabbro consists of amphibole, plagioclase, minor clinocllore, and accessory chalcopyrite. Antipinite forms isometric and short prismatic crystals up to $0.1 \times 0.1 \times 0.15$ mm, and random aggregates up to 0.6 mm across. The new mineral is blue, translucent, with pale blue streak and a vitreous luster. It is brittle, with a Mohs hardness ~2. The cleavage is medium in three directions, which were not determined. $D_{\text{meas}} = 2.53(3)$ and $D_{\text{calc}} = 2.549$ g/cm³. Antipinite does not fluoresce under UV radiation. It is optically biaxial (+), $\alpha = 1.432(2)$, $\beta = 1.530(2)$, and $\gamma = 1.698(5)$ ($\lambda = 589$ nm); $2V_{\text{meas}} = 75(10)^\circ$; $2V_{\text{calc}} = 82^\circ$. Dispersion of optical axes is strong, $r < v$. The mineral is strongly pleochroic: Z (blue) > Y (light blue) > X (colorless). Antipinite dissolves in water, and its concentrated aqueous solution has a pH of 9. The main bands of the IR spectrum of antipinite (cm⁻¹) are: weak bands over 1800 (combination modes), 1500–1750 (asymmetric stretching vibrations of carboxylate groups), 1280–1490 (their symmetric stretching vibrations), 780–900 (in-plane bending vibrations of the carboxylate groups, possibly combined with C-C stretching vibrations), 495–557 (out-of-plane bending vibrations of the carboxylate groups). No absorption bands associated with H₂O molecules, C-H bonds, CO₃²⁻, NO₃⁻, and OH⁻ ions were observed. The averaged 5 point EDS elec-

tron probe analyses is [wt%, (range)]: Na 11.83 (11.42–12.24), K 6.35 (5.97–6.95), Cu 21.84 (21.34–22.18), C (by gas chromatography) 16.22; total for all cations 56.24. The empirical formula of antipinite $\text{K}_{0.96}\text{Na}_{3.04}\text{Cu}_{2.03}(\text{C}_{2.00}\text{O}_4)_4$ based on 16 O pfu. The strongest lines of the X-ray powder diffraction pattern are [d_{obs} Å ($I_{\text{obs}}\%$; hkl)]: 5.22 (40; $\bar{1}\bar{1}1$), 3.47 (100; 032), 3.39 (80; $\bar{2}10$), 3.01 (30; 033,220), 2.543 (40; 122,034,104), 2.481 (30; $\bar{2}13$), 2.315 (30; $\bar{1}\bar{4}3,310$), 1.629 (30; $\bar{1}\bar{4}6,414,243,160$). The crystal structure of antipinite was determined by “charge-flipping” method and refined to $R = 3.27\%$. It is triclinic, $P\bar{1}$, $a = 7.1574(5)$, $b = 10.7099(8)$, $c = 11.1320(8)$ Å, $\alpha = 113.093(1)$, $\beta = 101.294(1)$, $\gamma = 90.335(1)^\circ$, $V = 766.5(1)$ Å³, and $Z = 2$. The crystal structure consists of planar C₂O₄ units, a layer of Na atoms and a layer of Cu atoms with pairs of K atoms. The C₂O₄ and Na-Cu-K layers are coplanar with the (001) plane and are joined by an O atom shared with oxalate groups. Antipinite is the only known anhydrous Cu oxalate containing both Na and K. The type specimen is deposited in the Technische Universität, Bergakademie Freiberg, Germany. **Yu.U.**

ANZAITE-(CE)*

A.R. Chakhmouradian, M.A Cooper, L. Medici, Y.A. Abdu and Y.S. Shelukhina (2015) Anzaite-(Ce), a new rare-earth mineral and structure type from the Afrikanda silicocarbonatite, Kola Peninsula, Russia. Mineralogical Magazine, 79(5), 1231–1244.

Anzaite-(Ce) (IMA 2013-004), ideally $\text{Ce}_3^+\text{Fe}^{2+}\text{Ti}_6\text{O}_{18}(\text{OH})_2$, is a new REE mineral from hydrothermally altered silicocarbonatites in the Afrikanda alkali-ultramafic complex, Kola Peninsula, Russia. The new mineral honors Anatoly Zaitsev (b. 1963), Professor of Mineralogy at St. Petersburg State University for his contributions to the studies of REE minerals, carbonatites and alkaline rocks of the Kola Peninsula. Anzaite-(Ce) occurs in association with titanite, hibschite, clinocllore, and calcite, replacing the primary magmatic ilmenite and/or Ti-rich magnetite of the calcite-amphibole-clinopyroxene silicocarbonatite. It forms sub- to euhedral crystals of elongate prismatic habit and a diamond-like cross section less than 100×15 μm in size. Anzaite-(Ce) is grayish black, opaque, brittle, has a submetallic

* All minerals marked with an asterisk have been approved by the IMA CNMMC.
† For a complete listing of all IMA-validated unnamed minerals and their codes, see <http://pubsites.uws.edu.au/ima-cnmmc/>.

luster, and no cleavage. Hardness and density were not measured due to the small size of crystals and scarcity of material; $D_{\text{calc}} = 5.054 \text{ g/cm}^3$. It does not fluoresce under UV radiation. In reflected light, anzaite-(Ce) is gray with a slight bluish hue; bireflectance is weak. The interpolated reflectance values (in air) [R_{min} , R_{max} (nm)] are: 14.8, 15.7 (440); 13.9, 15.1 (460); 13.8, 14.8 (470); 13.8, 14.6 (480); 13.8, 14.7 (500); 13.4, 14.9 (520); 13.0, 14.8 (540); 13.0, 14.8 (546); 12.9, 14.7 (560); 12.8, 14.3 (580); 13.0, 14.3 (589); 13.1, 14.3 (600); 13.3, 14.2 (620); 13.3, 14.3 (640); 13.2, 14.2 (650); 13.0, 14.1 (660); 13.1, 13.9 (680); 13.0, 14.2 (700). IR spectroscopy identified a sharp absorption band at $\sim 3475 \text{ cm}^{-1}$ assigned to the presence of OH groups. The average of 10 electron probe WDS analyses is [(wt%, (range))]: Nb₂O₅ 2.31 (0.77–3.47), TiO₂ 36.52 (35.68–37.44), SiO₂ 0.17 (0.04–0.28), ThO₂ 0.14 (0–0.33), La₂O₃ 5.40 (4.85–6.96), Ce₂O₃ 28.73 (26.65–31.52), Pr₂O₃ 3.42 (3.04–3.80), Nd₂O₃ 11.54 (9.72–12.44), Sm₂O₃ 1.18 (0.76–1.40), CaO 1.64 (1.12–2.48), FeO 5.63 (5.41–5.84), H₂O (calc) 1.45, total 98.13. The formula calculated on the basis of 20 (O+OH) pfu is: (Ce_{2.18}Nd_{0.85}La_{0.41}Pr_{0.26}Sm_{0.08}Ca_{0.36}Th_{0.01})_{Σ4.15}Fe_{0.97}(Ti_{5.68}Nb_{0.22}Si_{0.04})_{Σ5.94}O₁₈(OH)_{2.00}. The strongest lines of the X-ray powder diffraction pattern [$d \text{ \AA}$ ($I\%$; hkl)] are: 2.596 (100; 002), 1.935 (18; 170), 1.506 (14; 133), 1.286 (13; 1.11.0), 2.046 (12; $\bar{2}41$), 1.730 (12; 003), 1.272 (12; 0.10.2), 3.814 (11; $\bar{1}11$), 2.206 (9; 061), 1.518 (9; 172). Anzaite-(Ce) is monoclinic, space group $C2/m$, $a = 5.290(2)$, $b = 14.575(6)$, $c = 5.234(2) \text{ \AA}$, $\beta = 97.233(7)^\circ$, $V = 400.4 \text{ \AA}^3$, $Z = 1$. The crystal structure of anzaite-(Ce) was solved and refined to $R_1 = 2.1\%$. It consists of two alternating layers. The layer of type 1 is composed of REE (+minor Ca) in a square antiprismatic coordination and octahedrally coordinated Fe²⁺, while the layer of type 2 is built of [5]- and [6]-coordinated Ti polyhedra stacked parallel to (001). Octahedrally coordinated Fe²⁺, [5]- and [6]-coordinated Ti, and two out of the four anion sites are disordered so that only one half of these positions occupy any given (010) plane. Anzaite-(Ce) represents a new structure type. Due to its structural uniqueness it cannot be assigned to any of the existing mineral groups within REE-Ti oxides. Holotype and cotype specimens are deposited in the Robert B. Ferguson Museum of Mineralogy at the University of Manitoba, Winnipeg, Canada. **Yu.U.**

BETTERTONITE*

I.E. Grey, A.R. Kampf, J.R. Price and C.M. Macrae (2015) Bettertonite, [Al₆(AsO₄)₃(OH)₉(H₂O)₅]·11H₂O, a new mineral from the Penberthy Croft mine, St. Hilary, Cornwall, UK, with a structure based on polyoxometalate clusters. Mineralogical Magazine, 79(7), 1849–1858.

A new mineral bettertonite (IMA 2014-074), ideally [Al₆(AsO₄)₃(OH)₉(H₂O)₅]·11H₂O, was discovered at the Penberthy Croft mine in $\sim 1.5 \text{ km}$ from the village of Goldsithney, St. Hilary, Cornwall, England, U.K. (50.1414°N 5.4269°W). The mine is well known as a source of rare secondary CuPbFe arsenates and was classified in 1993 as an SSSI (Site of Special Scientific Interest). Bettertonite occurs in quartz veins closely associating with arsenopyrite, chamosite, liskeardite, pharmacalumite, pharmacosiderite and minor brochantite, chalcopyrite and cassiterite. Much of supergene alteration is post mining. The new mineral along with liskeardite was prob-

ably formed from leaching and the replacement of Al to Fe in pharmacosiderite. Bettertonite forms bright white, lustrous, ultra-thin (sub-micrometer) blades, sprays and laths with lateral dimensions $< 20 \text{ }\mu\text{m}$, or their radiating groups that line and infill interconnecting and isolated cavities (14 mm) in quartz and chamosite. The laths are flattened on {010}; other forms are {010}, {100}, and {001}. Bettertonite is translucent with a white streak and a vitreous to pearly or silky luster. The cleavage on {010} is perfect. The density was not measured due to the thinness of the crystals; $D_{\text{calc}} = 2.02 \text{ g/cm}^3$. The mineral is nonpleochroic, optically biaxial (+) with $\alpha = 1.511$, $\beta = 1.517$, $\gamma = 1.523$ (white light), $2V_{\text{calc}} = 60.2^\circ$; $X = \mathbf{c}$, $Y = \mathbf{b}$, $Z = \mathbf{a}$. The average of 4 electron probe WDS analyses [wt% (range)] is: Al₂O₃ 35.8 (34.5–36.1), Fe₂O₃ 2.45 (1.93–2.82), As₂O₅ 36.5 (35.6–37.7), SO₃ 2.19 (1.18–2.60), Cl 0.56 (0.29–0.89), O=Cl₂ 0.13, total 77.47. Normalized to a total of 100% when combined with the H₂O calculated based on structure analysis: Al₂O₃ 29.5, Fe₂O₃ 2.0, As₂O₅ 30.1, SO₃ 1.8, Cl 0.5, H₂O 36.2. The empirical formula, based on 9 (Al+Fe+As+S) pfu is Al_{5.86}Fe_{0.26}(AsO₄)_{2.65}(SO₄)_{0.23}(OH)_{9.82}Cl_{0.13}(H₂O)_{15.5}. The strongest lines in the powder X-ray diffraction pattern are [$d \text{ \AA}$ ($I\%$; hkl)]: 13.65 (100; 011), 13.51 (50; 020), 7.805 (50; 031), 7.461 (30; 110), 5.880 (20; 130), 3.589 (20; $\bar{2}02$); 2.857 (14; 182). The monoclinic unit-cell parameters refined in space group $P2_1/c$ from the powder X-ray data are $a = 7.788(3)$, $b = 26.957(7)$, $c = 15.925(8) \text{ \AA}$, $\beta = 93.9(1)^\circ$, $V = 3336 \text{ \AA}^3$. The refinement of single crystal data collected at 100 K on the microfocus beamline MX2 at the Australian Synchrotron ($\lambda = 0.71073 \text{ \AA}$) on a rectangular lath ($20 \times 10 \times 1 \text{ }\mu\text{m}$) yielded $R_1 = 0.083$ for 2164 observed [$I > 2\sigma(I)$] reflections. The single-crystal unit-cell parameters are: $a = 7.773(2)$, $b = 26.991(5)$, $c = 15.867(3) \text{ \AA}$, $\beta = 94.22(3)^\circ$, $V = 3319.9 \text{ \AA}^3$, $Z = 4$. Bettertonite is a natural example of a polyoxometalate (POM) compounds. It has a heteropolyhedral layered structure, with the layers parallel to (010). The layers comprise hexagonal rings of edge-shared AlO₆ octahedra that are interconnected by sharing corners with AsO₄ tetrahedra. The layers are strongly undulating and their stacking produces large channels along [100] that are filled with water molecules. These polyoxometalate clusters, of composition [AsAl₆O₁₁(OH)₉(H₂O)₅]⁸⁻, are interconnected along [100] and [001] by corner-sharing with other AsO₄ tetrahedra. The mineral honors John Betterton (b. 1959) a museum geologist/mineralogist at Haslemere Educational Museum, Haslemere, Surrey, U.K., for his extensive contributions to the characterization of minerals from the Penberthy Croft mine. Cotype specimens are deposited in the Museum Victoria, Melbourne, Victoria, Australia, and in the Natural History Museum, London, U.K. **D.B.**

BOBSHANNONITE*

E. Sokolova, F. Cámara, Y.A. Abdu, F.C. Hawthorne, L. Horváth and E. Pfenninger-Horváth (2015) Bobshannonite, Na₂KBa(Mn,Na)₈(Nb,Ti)₄(Si₂O₇)₄O₄(OH)₄(O,F)₂, a new TS-block mineral from Mont Saint-Hilaire, Québec: Description and crystal structure. Mineralogical Magazine, 79(7), 1791–1811.

The new mineral bobshannonite (IMA 2014052), ideally Na₂KBa(Mn,Na)₈(Nb,Ti)₄(Si₂O₇)₄O₄(OH)₄(O,F)₂, was discovered in the pegmatite from a blast pile at the Poudrette quarry, Mont

Saint-Hilaire, Québec, Canada. The type specimen is $2.5 \times 2.3 \times 2$ cm and consists mostly (~90%) of sérandite. Orange-brown blocky crystals of bobshannonite up to 0.51 mm are perched on sérandite and albite. Other associated minerals are epididymite (rich), catapleite, aegirine (2 generations), kupletskite, rhodochrosite, and rhabdophane-(Ce) and undetermined botryoidal Mn oxide. The mineral is of hydrothermal origin. The main forms of euhedral crystals of bobshannonite are $\{001\}$, $\{110\}$, $\{1\bar{1}0\}$, and $\{010\}$. The mineral is vitreous to frosty, transparent to translucent pale brown (in small fragments) to orange brown with a very pale brown streak and hackly fracture. Cleavage is perfect on $\{001\}$ and no parting was observed. It does not fluoresce under cathode or UV rays. The mineral is brittle with a Mohs hardness ~4. The density was not measured; $D_{\text{calc}} = 3.787 \text{ g/cm}^3$. Crystals of bobshannonite are extensively twinned and do not extinguish in cross-polarized light. That did not allow to obtain data on optical properties. The mineral is non pleochroic in the cleavage plain, but change color from colorless to brown in other sections. The FTIR and Raman spectra show a strong peak at 3610 with a weak shoulder at 3655 cm^{-1} assigned to the stretching vibrations of OH groups. A strong peak at 901 cm^{-1} and medium- to low-intensity peaks at 1038, 970, 716, and 680 cm^{-1} on the Raman spectrum may be assigned to Si–O stretching vibrations of the Si_2O_7 groups. Peaks at 608, 580, 510, and 410 cm^{-1} correspond to bending vibrations of Si_2O_7 groups and those at 341, 310, 240, 207, and 143 cm^{-1} to the lattice modes. The average of 9 electron probe WDS analysis (ranges are not given) is (wt%): Ta_2O_5 0.52, Nb_2O_5 19.69, TiO_2 5.50, SiO_2 26.31, Al_2O_3 0.06, BaO 7.92, ZnO 1.02, FeO 0.89, MnO 26.34, MgO 0.06, Rb_2O 0.42, K_2O 2.38, Na_2O 4.05, F 0.70, H_2O (calculated using structure data) 1.96, $\text{O}=\text{F}_2$ 0.29, total 97.53. The empirical formula based on 38 (O+F) is $\text{Na}_{1.89}(\text{K}_{0.93}\text{Rb}_{0.08})_{\Sigma 1.01}\text{Ba}_{0.95}(\text{Mn}_{6.85}\text{Na}_{0.52}\text{Zn}_{0.23}\text{Fe}_{0.23}^{2+}\text{Mg}_{0.03}\text{Al}_{0.02})_{\Sigma 7.88}(\text{Nb}_{2.73}\text{Ti}_{1.27}\text{Ta}_{0.04})_{\Sigma 4.04}(\text{Si}_{8.07}\text{O}_{28})\text{O}_{9.32}\text{H}_{4.01}\text{F}_{0.68}$. The strongest lines in the powder X-ray diffraction pattern [d Å ($P\%$; hkl)] are: 2.873 (100; $\bar{2}\bar{4}1, \bar{2}\bar{4}1, 044, 0\bar{4}\bar{4}, 241, \bar{2}\bar{4}1$), 3.477 (60; 006), 3.193 (59; $224, \bar{2}\bar{2}\bar{4}$), 2.648 (40; $\bar{4}02, 243, \bar{2}\bar{4}3$), 2.608 (35; 008, $226, \bar{2}\bar{2}6$), 1.776 (30; 249). The triclinic unit-cell parameters (space group $C\bar{1}$) refined from the powder X-ray data are $a = 10.826(5)$, $b = 13.896(6)$, $c = 20.946(7)$ Å, $\alpha = 90.00(3)$, $\beta = 95.01(3)$, $\gamma = 90.00(3)^\circ$, $V = 3139 \text{ \AA}^3$. The single crystal unit-cell parameters are $a = 10.839(6)$, $b = 13.912(8)$, $c = 20.98(1)$ Å, $\alpha = 89.99(1)$, $\beta = 95.05(2)$, $\gamma = 89.998(9)^\circ$, $V = 3152 \text{ \AA}^3$, $Z = 4$. The crystal structure was refined to $R_1 = 2.55\%$ for the space group $C\bar{1}$ on the basis of 7277 unique [$F > 4\sigma(F)$] reflections and can be described as a combination of a titanium silicate (TS) block and an I (Intermediate) block. The TS block consists of HOH sheets (H = heteropolyhedral, O = octahedral). The topology of the TS block is as in Group II of the Ti disilicates: $\text{Ti} + \text{Nb} = 2$ apfu per $(\text{Si}_2\text{O}_7)_2$ (Sokolova, 2006). In the O sheet, ten M^O octahedra form a close-pack and are occupied mainly by Mn, less Na and minor Zn, Fe^{2+} , Mg, and Al. The Si_2O_7 groups and M^H octahedra occupied by Nb and Ti ($\text{Nb} > \text{Ti}$) share common vertices to form the two identical H sheets. An O sheet and two adjacent H sheets link through common vertices of SiO_4 tetrahedra and M^H and M^O octahedra to form a TS block parallel to (001). The TS blocks link via common vertices of M^H octahedra. In the I block, Ba and K are ordered at the peripheral $A^P(1)$ and $A^P(2)$ sites with $\text{Ba}:\text{K} = 1:1$ and the two B^P sites are occupied by Na. The ideal

composition of the I block is Na_2KBa apfu. Bobshannonite, perraultite, surkhobite, and jinshajiangite are topologically identical Group-II TS -block minerals. Bobshannonite is the Nb-analog of perraultite. The mineral honors Robert (Bob) D. Shannon (b. 1935), in recognition of his major contributions to the fields of crystal chemistry and mineralogy through his development of accurate and comprehensive ionic radii and his work on dielectric properties of minerals. The holotype specimen has been deposited at the Canadian Museum of Nature, Ottawa, Canada. **D.B.**

References cited

Sokolova, E. (2006) From structure topology to chemical composition. I. Structural hierarchy and stereochemistry in titanium disilicate minerals. *Canadian Mineralogist*, 44(6), 1273–1330.

CALCINAKSITE*

N.V. Chukanov, S.M. Aksenov, R.K. Rastsvetaeva, G. Blass, D.A. Varlamov, I.V. Pekov, D.I. Belakovskiy and V.V. Gurzhii (2015) Calcinaksite, $\text{KNaCa}(\text{Si}_4\text{O}_{10})\text{H}_2\text{O}$, a new mineral from the Eifel volcanic area, Germany. *Mineralogy and Petrology*, 109, 397–404.

Calcinaksite (IMA 2013-081), ideally $\text{KNaCa}(\text{Si}_4\text{O}_{10})_2 \cdot \text{H}_2\text{O}$, is a new mineral found in a xenolith of metamorphosed carbonate-rich rock from the southern lava flow of the Bellerberg volcano, Eastern Eifel region, Rheinland-Pfalz, Germany. It is named for its chemical composition and by analogy with manaksite and fenaksite, Mn and Fe end-members. The new mineral occurs in association with wollastonite, gehlenite, brownmillerite, calcio-olivine, quartz, aragonite, calcite, jennite, tobermorite, and ettringite. Calcinaksite forms clusters of subhedral prismatic crystals that are elongated along a , up to 1 cm long and embedded with wollastonite, gehlenite, and other calcium silicates. It is colorless to light gray, brittle, with a Mohs hardness of 5. Calcinaksite has two perfect cleavages on $\{001\}$ and $\{010\}$. $D_{\text{meas}} = 2.62(2)$ and $D_{\text{calc}} = 2.623 \text{ g/cm}^3$. Calcinaksite does not fluoresce in both UV and cathode rays. It is biaxial (+), with $\alpha = 1.542(2)$, $\beta = 1.550(2)$, $\gamma = 1.565(2)$ ($\lambda = 589 \text{ nm}$), $2V_{\text{meas}} = 75(10)^\circ$; $2V_{\text{meas}} = 73^\circ$; $Y \wedge a = 42^\circ$, $Z \wedge a \approx 90^\circ$. Dispersion of optical axes is medium, $r < v$. The main bands of the IR spectrum are (cm^{-1} , s = strong, w = weak, sh = shoulder): 3540, 3340w, 3170w (O–H stretching vibrations of H_2O molecules), 1654w (bending vibrations of H_2O molecules), 1122, 1075sh, 1055sh, 1041s, 1013, 971s (Si–O stretching vibrations), 775w, 679, 624, 597, 523 (bending vibrations of the tubular silicate radical Si_4O_{10}), 480sh, 456, 421s, 395w (lattice modes involving Si–O–Si bending and Ca–O stretching vibrations). The average of 18 electron probe EDS analyses is [(wt% (range))]: SiO_2 61.46 (60.83–62.08), FeO 0.59 (0–1.11), CaO 15.04 (14.15–15.66), K_2O 12.01 (11.21–12.64), Na_2O 6.69 (6.22–7.31), H_2O 4.9 (two measurements 4.72 and 5.05 by the Alimarin method), total 100.69. The formula calculated based on 11 O atoms pfu is: $\text{K}_{0.99}\text{Na}_{0.84}\text{Ca}_{1.04}\text{Fe}_{0.03}\text{Si}_{3.98}\text{O}_{11}$. The strongest lines of the X-ray powder diffraction pattern [d Å ($P\%$; hkl)] are: 3.431 (70; $\bar{1}21, \bar{2}11, \bar{2}10, 012, 0\bar{2}2$), 3.300 (67; $0\bar{1}3$), 3.173 (95; $\bar{1}03, \bar{2}01, \bar{2}20, 003, 111$), 3.060 (100; $\bar{2}12, \bar{2}\bar{1}1, \bar{2}21, 200, \bar{1}\bar{1}3, 021, \bar{2}02$), 2.851 (83; $0\bar{2}3, \bar{1}22, 1\bar{1}3, 1\bar{1}1$), 2.664 (62; $\bar{1}23, \bar{2}22, 201$). The crystal structure of calcinaksite was refined to $R_1 = 5.3\%$. The mineral is triclinic, $P\bar{1}$, $a = 7.021(2)$, $b = 8.250(3)$, $c = 10.145(2)$ Å, $\alpha = 102.23(2)$, $\beta = 100.34(2)$, γ

= 115.09(3)°, $V = 495.4(3) \text{ \AA}^3$, and $Z = 2$. The crystal structure of calcinaksite is based on an infinite $[\text{Si}_8\text{O}_{20}]^{8-}$ tube running along [100]. The lateral plane of the tube consists of [4]- and [8]-membered tetrahedral rings. The tubes are joined by edge-sharing $[\text{CaO}_5(\text{H}_2\text{O})]$ square bipyramids and $[\text{NaO}_5]$ polyhedral. The K atoms occupy large cavities within $[\text{Si}_8\text{O}_{20}]^{8-}$ tubes. The type specimen is housed in the Fersman Mineralogical Museum, Russian Academy of Sciences, Moscow, Russia. **Yu.U.**

KHVOROVITE*

L.A. Pautov, A.A. Agakhanov, E.V. Sokolova, F.C. Hawthorne, V.Yu. Karpenko, O.I. Siidra, V.K. Garanin and Y.A. Abdu (2015) Khvorovite, $\text{Pb}_4^{2+}\text{Ca}_2[\text{Si}_8\text{B}_2(\text{SiB})\text{O}_{28}]\text{F}$, a new hyalotekite-group mineral from the Darai-Pioz alkaline massif, Tajikistan: Description and crystal structure. *Mineralogical Magazine*, 79(4), 949–963.

Khvorovite (IMA 2014-050), ideally $\text{Pb}_4^{2+}\text{Ca}_2[\text{Si}_8\text{B}_2(\text{SiB})\text{O}_{28}]\text{F}$, is a new mineral found at the Darai-Pioz alkaline massif in the upper reaches of the Darai-Pioz river, Tajikistan. Khvorovite occurs in a pectolite aggregate in silexites where the aggregate consists mainly of pectolite, quartz, and fluorite, with minor aegirine, polyolithionite, turkestanite, and baratovite. Accessory minerals include calcite, pyrochlore-group minerals, reedmergnite, stillwellite-(Ce), pekovite, zeravshanite, senkevichite, sokolovaite, mendeleevite-(Ce), alamosite, orlovite, leucosphenite, and several unknown Cs-silicates. Khvorovite occurs as irregular grains, rarely with square or rectangular sections up to 150 μm , and grain aggregates up to 0.5 mm. The mineral is colorless (rarely white), transparent with a white streak and a vitreous luster. It shows no cleavage or parting and is brittle with an uneven fracture. The micro indentation hardness $\text{VHN} = 620$ (590–637) corresponding to 5–5½ of Mohs scale; $D_{\text{meas}} = 3.96(2)$ and $D_{\text{calc}} = 3.968 \text{ g/cm}^3$. Khvorovite is optically biaxial (+) with $\alpha = 1.659(3)$, $\beta_{\text{calc}} = 1.671(2)$, $\gamma = 1.676(3)$ ($\lambda = 589 \text{ nm}$); $2V_{\text{meas}} = 64(3)^\circ$; dispersion of optical axes is medium $r < v$. The mineral does not fluoresce under UV light but fluoresces pale blue under the electron beam. The Raman spectrum shows peaks at 1100, 1017, and 937 cm^{-1} (Si-O and B-O stretches), 783, 713 and 642 cm^{-1} (stretching vibrations of Si-O-Si bridges), 531, 485, and 425 cm^{-1} (bending vibrational modes of SiO_4 tetrahedra), and below 400 cm^{-1} (lattice modes). The average of 10 electron probe EDS analyses (for boron WDS was used) is [wt% (range)]: SiO_2 36.98 (36.36–37.78), B_2O_3 6.01 (5.40–6.10), Y_2O_3 0.26 (0–0.64), PbO 40.08 (37.24–42.49), BaO 6.18 (4.05–8.96), SrO 0.43 (0–0.86), CaO 6.77 (6.01–7.37), K_2O 1.72 (1.39–2.05), Na_2O 0.41 (0.22–0.62), F 0.88 (0.63–1.10), $\text{O}=\text{F}$ 0.37, total 99.35. This gives the empirical formula $(\text{Pb}_{2.76}^{2+}\text{Ba}_{0.62}\text{K}_{0.56}\text{Na}_{0.16})_{\Sigma 4.10}(\text{Ca}_{1.86}\text{Sr}_{0.06}\text{Y}_{0.04}\text{Na}_{0.04})_{\Sigma 2}[\text{Si}_8\text{B}_2(\text{Si}_{1.46}\text{B}_{0.65})_{\Sigma 2.11}\text{O}_{28}](\text{F}_{0.71}\text{O}_{0.29})$ based on 29 O+F. The strongest lines in the X-ray powder-diffraction pattern [$d \text{ \AA}$ ($I\%$; hkl)] are: 7.86 (100; 110), 7.65 (90; $\bar{1}01$), 7.55 (90; 011), 3.81 (90; 202), 3.55 (90; 301), 2.934 (90; $\bar{3}\bar{1}2$, 312). The unit-cell parameters refined from powder-diffraction data are: $a = 11.35(2)$, $b = 10.97(3)$, $c = 10.28(3) \text{ \AA}$, $\alpha = 90.27(4)$, $\beta = 89.97(4)$, $\gamma = 89.98(4)^\circ$, $V = 1280 \text{ \AA}^3$. Single-crystal X-ray diffraction data collected on a crystal of size 0.020×0.025×0.030 mm refined to $R_1 = 2.89$ for 3751 unique $I \geq 4\sigma(I)$ reflections shows khvorovite is triclinic, space group $\bar{1}I$, $a = 11.354(2)$,

$b = 10.960(2)$, $c = 10.271(2) \text{ \AA}$, $\alpha = 90.32(3)$, $\beta = 90.00(3)$, $\gamma = 90.00(3)^\circ$, $V = 1278 \text{ \AA}^3$, $Z = 2$. Khvorovite is a Pb^{2+} analog of hyalotekite, and a Pb^{2+} and Ca analog of kapitsaite-(Y). Its structure consists of Si, B tetrahedra that form an interrupted framework of ideal composition $[\text{Si}_8\text{B}_2(\text{SiB})\text{O}_{28}]^{11-}$ with interstitial cations Pb^{2+} , Ba, K, and Ca in the channels within the framework. Khvorovite is named in honor of Pavel Vitalyevich Khvorov (Павел Витальевич Хворов) (b. 1965), a Russian mineralogist for his contributions to the mineralogy of the Darai-Pioz massif. The holotype specimen is deposited in the Fersman Mineralogical Museum, Russian Academy of Sciences, Moscow, Russia. **O.C.G.**

LEGUERNITE*

A. Garavelli, D. Pinto, D. Mitolo and L. Bindi (2015) Leguernite, $\text{Bi}_{12.67}\text{O}_{14}(\text{SO}_4)_5$, a new Bi oxysulfate from the fumarole deposit of La Fossa crater, Vulcano, Aeolian Islands, Italy. *Mineralogical Magazine*, 78(7), 1629–1645

Leguernite (IMA 2013-051), ideally $\text{Bi}_{12.67}\text{O}_{14}(\text{SO}_4)_5$, is a new mineral found at La Fossa crater, Vulcano, Aeolian Islands, Italy. The mineral was found in a cavity of a volcanic rock sample from the walls of the high-temperature fumarole FF ($T = 600 \text{ }^\circ\text{C}$) closely associated with anglesite, baličžuničite, and an unknown Bi sulfate. Other associated minerals include lillianite, galenobismutite, bismoclite, Cd-rich sphalerite, Cd-rich wurtzite, pyrite, and pyrrhotite. It occurs as fibrous aggregates of needle-shaped crystals up to 0.4 × 0.01 mm. Leguernite is colorless to white, transparent with white streak and subadamantine luster. It is brittle, shows no cleavage, parting, or fractures. No twinning was observed. Hardness, density and refractive indices were not measured due to size and paucity of material; $D_{\text{calc}} = 7.375 \text{ g/cm}^3$. The mineral does not fluoresce under UV light. The Raman spectrum shows peaks in the region 600–1200 cm^{-1} (SO_4 stretching modes) and 400–600 cm^{-1} (SO_4 bending modes). Most of the bands in the region 100–400 cm^{-1} are due to the Bi-O lattice vibrations. A peak at 2430 cm^{-1} remains unassigned. No peaks confirming the presence of OH or H_2O groups were observed. The average of 9 electron probe EDS analyses on different crystals belonging to the same needle aggregate is [wt% (range)]: SO_3 11.06 (10.76–11.29), Bi_2O_3 78.57 (75.80–80.03), PbO 0.91 (0.36–1.63) total 90.54. This gives the empirical formula $(\text{Bi}_{12.40}\text{Pb}_{0.15})_{\Sigma 12.55}\text{S}_{5.08}\text{O}_{34}$ based on 34 anions pfu. The strongest lines in the X-ray powder-diffraction pattern [$d \text{ \AA}$ ($I\%$; hkl)] are: 3.220 (100; 013), 3.100 (95; $\bar{3}11$), 2.83 (30; 020), 2.931 (25; 302), 2.502 (25; $\bar{3}04$), 2.035 (20; 322), 1.875 (20; $\bar{3}24$), and 5.040 (15; 110). The unit-cell parameters refined from powder-diffraction data are: $a = 11.250(5)$, $b = 5.654(2)$, $c = 11.906(5) \text{ \AA}$, $\beta = 99.13(5)^\circ$, and $V = 747.8 \text{ \AA}^3$. Single-crystal X-ray diffraction data collected on a crystal of size 0.260×0.034×0.016 mm refined to $R_1 = 0.0766$ for 2372 unique $I \geq 4\sigma(I)$ reflections shows leguernite is monoclinic, space group $P2_1$, with $a = 11.2486(11)$, $b = 5.6568(6)$, $c = 11.9139(10) \text{ \AA}$, $\beta = 99.177(7)^\circ$, $V = 748.39 \text{ \AA}^3$, $Z = 1$. The crystal structure of leguernite consists of (001) layers with composition $[\text{Bi}_{12}\text{O}_{14}(\text{SO}_4)]_n^{6+}$ alternating with layers of composition $[\text{Bi}(\text{SO}_4)_4]_n^{5-}$ along [001]. Bi-O blocks are of a fluorite-like structure with $\text{Bi}_{12}\text{O}_{14}$ composition separated by a single sulfate ion along [100] and by $\text{Bi}(\text{SO}_4)_4^-$ groups along [101]. Leguernite is

named in honor of François Le Guern (1942–2011), better known as “Fanfan,” a very active volcanologist and expert on volcanic gases and sublimates. The holotype specimen is deposited in the Museum “C.L. Garavelli,” Dipartimento di Scienze della Terra e Geoambientali, Università di Bari, Italy. **O.C.G.**

LUKKULAISSVAARAITE*

A. Vymazalová, T.L. Grokhovskaya, F. Laufek and V.A. Rassulov (2014) Lukkulaissvaaraite, $\text{Pd}_{14}\text{Ag}_2\text{Te}_9$, a new mineral from Lukkulaissvaara intrusion, northern Russian Karelia, Russia. *Mineralogical Magazine*, 78(7), 1743–1754.

Lukkulaissvaaraite (IMA 2013-015), ideally $\text{Pd}_{14}\text{Ag}_2\text{Te}_9$, is a new mineral found at the Lukkulaissvaara intrusion, northern Karelia, Russia. The mineral occurs with other platinum group element (PGE) minerals in gabbro-norite from the Early Proterozoic Lukkulaissvaara layered intrusion. The mineral formed under post-magmatic conditions below 600 °C and was found rimmed by tulameenite and accompanied randomly by telargpalite and Bi-rich kotulskite, enclosed within chalcopyrite in association with millerite, bornite, hematite, moncheite, tulameenite, hongshiite, telluropalladinite, sperrylite, palarstanide, and polymineralic platinum-group mineral grains. Lukkulaissvaaraite is opaque with gray streak, a metallic luster and is brittle. The micro-indentation hardness $\text{VHN}_{20} = 355$ (339–371) kg/mm^2 , corresponds to ~4 of a Mohs scale. In plane-polarized light, lukkulaissvaaraite is light gray with a brownish tinge, has strong birefractance, light brownish-gray to grayish-brown pleochroism. Anisotropy is distinct to strong. No internal reflections were observed. Reflectance values were measured in air between 400 and 700 nm in 20 nm intervals. The values for COM wavelengths [R_{\min} , R_{\max} % (λ nm)] are: 40.9, 48.3 (470); 47.6, 56.4 (546); 52.1, 61.0 (589); 57.5, 65.2 (650). The average of 5 electron probe WDS analyses is [wt% (range)]: Pd 52.17 (51.06–53.27), Ag 7.03 (6.26–7.69), Te 40.36 (39.77–41.23), Bi 0.05 (0.03–0.09), total 99.61. This gives the empirical formula $\text{Pd}_{14.05}\text{Ag}_{1.88}\text{Te}_{9.06}$ based on 25 apfu. The strongest lines in the X-ray powder-diffraction pattern of synthetic lukkulaissvaaraite [d Å ($I\%$; hkl)] are: 2.832 (58; 130,310), 2.809 (92; 213), 2.554 (66; 312), 2.431 (41; 321,231), 2.137 (57; 411,141), 2.1015 (52; 233,323), 2.045 (100; 314), 2.003 (63; 420,240), 1.970 (30; 006), 1.405 (30; 246,426), 1.319 (36; 543,453). The crystal structure was solved and refined from the powder X-ray diffraction (XRD) data of synthetic $\text{Pd}_{14}\text{Ag}_2\text{Te}_9$. The mineral is tetragonal, space group $I4/m$, with $a = 8.9599(6)$, $c = 11.822(1)$ Å, $V = 949.1$ Å³, and $Z = 2$. Lukkulaissvaaraite has a unique structure type and shows similarities to that of sopcheite ($\text{Ag}_4\text{Pd}_3\text{Te}_4$) and palladseite ($\text{Pd}_{17}\text{Se}_{15}$). The structure can be viewed as a three-dimensional framework composed of two types of blocks of polyhedra interconnected by common Te atoms. There are four independent metal sites (M1–M4) and two Te sites where M(1) can be viewed as in transition between tetrahedral and square planar, M(2) and M(3) are at the centers of rectangles formed by Te atoms and where M(4) site is surrounded by four M(1) and four M(2) sites in a distorted square antiprismatic coordination. The mineral is named for the type locality. The holotype is deposited in the Department of Mineralogy of the National Museum, Prague, Czech Republic. **O.C.G.**

MINJIANGITE*

- C. Rao, F. Hatert, R.C. Wang, X.P. Gu, F. Dal Bo and C.W. Dong (2015) Minjiangite, $\text{BaBe}_2(\text{PO}_4)_2$, a new mineral from Nanping No. 31 pegmatite, Fujian Province, southeastern China. *Mineralogical Magazine*, 79(5), 1195–1202.
- F. Dal Bo, F. Hatert, and M. Baijot (2014) Crystal chemistry of synthetic $\text{M}^{2+}\text{Be}_2\text{P}_2\text{O}_8$ ($\text{M}^{2+} = \text{Ca}, \text{Sr}, \text{Pb}, \text{Ba}$) berylllophosphates. *Canadian Mineralogist*, 52(2), 337–350.

Minjiangite (IMA 2013-021), ideally $\text{BaBe}_2(\text{PO}_4)_2$, is a new mineral found at in the Nanping No. 31 pegmatite, located in the southeastern margin of the Caledonian folded belt in the northwest Fujian Province, southeastern China (118°06' E, 26°40' N), where it occurs in the Be-rich secondary assemblages observed in the pegmatite. Rock samples of minjiangite were collected on the dumps from the mine opening at the 515 m level. Minjiangite crystals occur along fractures cutting montebrasite crystals altered during a late hydrothermal stage at which Ba and Sr were remobilized. Associated minerals mainly include quartz, muscovite, hydroxylapatite, and palermoite. Minjiangite also occurs as isolated grains included in an intimate mixture of muscovite, quartz, and hydroxylapatite. It forms subhedral to euhedral crystals, 5 to 200 μm long (usually 20 to 40 μm) and 5 to 50 μm wide. The mineral is white, transparent to translucent, with a vitreous luster. It does not exhibit fluorescence under short-wave (254 nm) and long-wave (366 nm) UV light. It is brittle with Mohs hardness ~6. No cleavage was observed. $D_{\text{calc}} = 3.49$ g/cm^3 . Optical data for minjiangite were measured on synthetic minjiangite obtained by Dal Bo et al. (2014), which is uniaxial (+), with $\omega = 1.587(3)$, $\epsilon = 1.602(2)$ ($\lambda = 589$ nm). Raman spectra of minjiangite show (cm^{-1}) a strong sharp peak at 1050 and a medium sharp peak 478 (stretching and bending modes of PO_4) medium sharp peaks at 1233, 491 (probable Be-O vibration modes), and weak sharp peaks at 328 and 189 (Ba-O bending vibrations). FTIR of minjiangite shows bands at 1375, 1363, 1339 (BeO_4 stretching), 1101, 1068, 1027 (PO_4 stretching), 781 and 730 (BeO_4 bending), in good agreement with data obtained by Dal Bo et al. (2014) for the synthetic material. Average of 8 electron probe WDS analyses is [wt% (range)]: P_2O_5 40.16 (39.51–40.78), BaO 43.01 (42.42–43.74), BeO 14.06 (by SIMS), SiO_2 0.17 (0–0.41), CaO 0.17 (0.02–0.37), SrO 0.08 (0.01–0.24), FeO 0.03 (0–0.07), MgO 0.01 (0–0.02), TiO₂ 0.07 (0.0–0.19), K₂O 0.05 (0.02–0.11), Na₂O 0.11 (0.06–0.13), total 97.92. The empirical formula, calculated on the basis of 8 O apfu is: $(\text{Ba}_{0.99}\text{Ca}_{0.01}\text{Na}_{0.01})_{\Sigma 1.01}\text{Be}_{1.98}(\text{P}_{1.99}\text{Si}_{0.01})_{\Sigma 2.00}\text{O}_8$. The strongest X-ray powder diffraction lines [d Å ($I\%$; hkl)] are: 3.763 (100; 101), 2.836 (81.3; 102), 2.515 (32.3; 110), 2.178 (25.6; 200), 2.162 (19; 103), 2.090 (63.9; 201), 1.770 (16.2; 113), 1.507 (25.4; 212). Unit-cell parameters calculated from the powder data are: $a = 5.030(8)$, $c = 7.467(2)$ Å, $V = 163.96$ Å³. Refinement of X-ray diffraction data collected on a single-crystal of the synthetic analog $\text{BaBe}_2(\text{PO}_4)_2$ yielded $R_{\text{all}} = 0.021$ for 120 unique reflections. Minjiangite is hexagonal, $P6/mmm$, with unit-cell parameters of $a = 5.029(1)$, $c = 7.446(1)$ Å, $V = 163.51$ Å³, $Z = 1$. Its crystal structure is topologically similar to that of the hexagonal feldspar dmisteinbergite ($\text{CaAl}_2\text{Si}_2\text{O}_8$). It is based on a double layer of tetrahedra containing both Be

and P, which are assembled in six-membered rings and stacked parallel to the *c* axis, forming channels. Tetrahedra are linked by sharing their apexes, forming a double layer; Ba atoms are located in 12-coordinated polyhedra occurring between two double layers. Be and P are disordered among the tetrahedra of the double layer in the synthetic analog. This disordered Be-P distribution is confirmed by the broad absorption bands observed in the infrared spectrum of minjiangite. The mineral is named after the Minjiang River, located near the Nanping pegmatite. The holotype specimen is deposited at the Geological Museum of China, Beijing, China, catalogue number M11842. A cotype of natural minjiangite is deposited at the Laboratory of Mineralogy, University of Liège (catalogue number 20390), as well as the synthetic crystal used for single-crystal structure determination (catalogue number 20386). **F.C.**

MÖHNITE*

N.V. Chukanov, S.M. Aksenov, R.K. Rastsvetaeva, I.V. Pekov, D.I. Belakovskiy and S.N. Britvin (2015) Möhnite, $(\text{NH}_4)_2\text{K}_2\text{Na}(\text{SO}_4)_2$, a new guano mineral from Pabellón de Pica, Chile. *Mineralogy and Petrology*, 109, 643–648.

Möhnite (IMA 2014-101), ideally $(\text{NH}_4)_2\text{K}_2\text{Na}(\text{SO}_4)_2$, is a new supergene mineral found in a guano deposit on the Pabellón de Pica mountain, near Chanabaya, Iquique Province, Tarapacá Region, Chile ($20^\circ55'S$, $70^\circ08'W$), which is of particular interest from the viewpoint of the behavior of copper in lithospheric processes, being the type locality of several N-bearing and organic copper minerals, where chalcopyrite served as source for copper. Associated minerals are salammoniac, halite, joanneumite, natroxalate, nitratine, chanabayaite, and a clay mineral. Möhnite crystals overgrow crystalline crusts of salammoniac and encrust cavities in salammoniac aggregates and form random aggregates and clusters (up to 1 mm across), as well as crusts consisting of imperfect bipyramidal, light brown to brown spindle-shaped crystals up to $0.07 \times 0.07 \times 0.15$ mm in size. It does not exhibit fluorescence under UV light. It is brittle with no cleavage observed and Mohs hardness is 3. $D_{\text{meas}} = 2.4(1)$ (measured by flotation in heavy liquids) and $D_{\text{calc}} = 2.461$ g/cm³. Möhnite dissolves in water but is stable in dry air. Under plane-polarized light möhnite is light brownish-yellow and non-pleochroic. In crossed nicols it looks isotropic. The mineral is optically neutral, with ϵ and $\omega = 1.505(2)$ ($\lambda = 589$ nm). FTIR spectrum of möhnite shows bands at (cm⁻¹; s = strong, m = medium; w = weak): 3240m, 3076m, 2150w, 2078w, 1431, 1165s, 1111s, 988m, 836w, 775w, 619s, 555w, 519w, 450w. Band assignment are in agreement with the presence of NH_4^+ and SO_4 groups. Bands in the range from 1500 to 1700 cm⁻¹ that could belong to H_2O molecules are absent in the IR spectrum of möhnite. Average of electron probe EDS analyses (using rastered 8×8 μm beam; number of analyses not reported) is [wt% (range)]: $(\text{NH}_4)_2\text{O}$ 7.99 (N by gas chromatography, H by stoichiometry), Na_2O 9.49 (8.98–9.94), K_2O 32.34 (31.89–32.79), SO_3 51.32 (50.76–51.92), total 101.14 wt%. The empirical formula, calculated on the basis of 8 O apfu is: $(\text{NH}_4)_{0.95}\text{Na}_{0.95}\text{K}_{2.14}\text{S}_{1.99}\text{O}_8$. The strongest X-ray powder diffraction lines [d Å ($I\%$; hkl)] are: 4.955 (27; 100), 4.122 (37; 101,011), 3.708 (29; 002), 2.969 (74; 102,012), 2.861 (100; 110), 2.474 (20; 003), 2.060 (33; 022). Unit-cell parameters

refined from the powder data are: $a = 5.732(1)$, $c = 7.425(1)$ Å, $V = 211.3$ Å³. Refinement of X-ray diffraction data collected on a single-crystal ($0.11 \times 0.13 \times 0.15$ mm) yielded $R_1 = 0.0492$ for 241 unique $F > 4\sigma(F)$ reflections. Möhnite is trigonal, $P\bar{3}m1$, with unit-cell parameters of $a = 5.7402(3)$, $c = 7.435(1)$ Å, $V = 212.16$ Å³, $Z = 1$. Möhnite belongs to the apthitalite group and is isostructural with apthitalite, $\text{K}_3\text{Na}(\text{SO}_4)_2$. The fundamental building block of the apthitalite structure is a layer consisting of vertex-connected NaO_6 regular octahedra and SO_4 tetrahedra. Larger cations (NH_4^+ and K) are ordered in two sites (a 10-vertex and a 12-vertex polyhedra), one of which is attached to the layer; the other is situated between the layers. Möhnite is the first NH_4^+ -dominant member of the apthitalite group. A mineral with 5.68 wt% $(\text{NH}_4)_2\text{O}$ and 33.87 wt% K_2O from the Guañape Islands, Peru, was described by Frondel (1950) as an ammonium variety of apthitalite. The crystal structure of this mineral was not investigated, but according to chemical data it may be an ammonium-deficient variety of möhnite. The mineral is named in honor of the prominent German amateur mineralogist and mineral collector Gerhard Möhn (b. 1959), coauthor of descriptions of several new mineral species. The holotype specimen is deposited in the Fersman Mineralogical Museum of the Russian Academy of Sciences, Moscow, Russia. **F.C.**

References cited

Frondel, C. (1950) Notes on arcanite, ammonian apthitalite and oxammitte. *American Mineralogist*, 35, 596–598.

MORASKOITE*

Ł. Karwowski, J. Kusz, A. Muszyński, R. Kryza, M. Sitarz and E.V. Galuskin (2015) Moraskoite, $\text{Na}_2\text{Mg}(\text{PO}_4)\text{F}$, a new mineral from the Morasko IAB-MG iron meteorite (Poland). *Mineralogical Magazine*, 79(2), 387–398

Moraskoite (IMA 2013-084), ideally $\text{Na}_2\text{Mg}(\text{PO}_4)\text{F}$, is a new mineral found in the Morasko IAB-MG iron meteorite. Moraskoite occurs in a graphite-troilite inclusion that is rimmed by a schreibersite-cohenite halo, enclosed in a kamacite-taenite matrix, and is interpreted as being a primary phosphate. Associated minerals include chlorapatite, buchwaldite, brianite, merillite, a new phosphate phase of composition $\text{Na}_4\text{MgCa}_3(\text{PO}_4)_4$, chromite, enstatite (bronzite), kosmochlor, kosmochlor-augite, olivine, albite, orthoclase, quartz, cohenite, schreibersite, nickel phosphide, altaite, pyrrhotite, sphalerite, daubreelite, djerfischerite, whitlockite, and native Cu. Moraskoite forms aggregates up to 1.5 mm, with individual grains of irregular shape 20–300 μm across, and also occurs in smaller single grains intergrown with buchwaldite and filled with numerous graphite inclusions. Moraskoite is colorless and transparent with a white streak and vitreous luster. It has irregular, conchoidal fracture, and rarely observed cleavage. The density was not measured because of the small grain size and intimate intergrowth with graphite; $D_{\text{calc}} = 2.925$ g/cm³. Mohs hardness is 4–5. The wedge-shaped form of the grains did not allow the exact determination of optical constants. The mineral is non-pleochroic, optically biaxial, with very low birefringence (~ 0.004) and small $2V$ angle. The refractive index measured in a random cross-section is 1.550(4) ($\lambda = 589$ nm). Fluorescence is weak blue in UV radiation (254

and 360 nm). The Raman spectrum shows bands (cm^{-1}) at 1114 (ν_3 antisymmetric stretching vibrations of PO_4^{3-}), 1027, 962 (ν_1 antisymmetric stretching vibrations of PO_4^{3-}), 589 (ν_4 bending mode of PO_4^{3-}), 438 (ν_2 bending mode of PO_4^{3-}), 336, 308 (Mg-O/F stretching vibrations), 279, 262, 244, 193, 184, 147, and 131 (external vibrations). The Raman data shows the absence of H_2O and CO_2 . The average of 77 electron probe WDS analyses is [wt% (range)]: P_2O_5 38.79 (36.53–40.88), MgO 23.51 (20.92–26.56), FeO 0.53 (0.12–1.21), MnO 0.06 (0.00–0.35), Na_2O 31.92 (30.07–33.66), F 10.40 (9.59–11.40), $\text{O}=\text{F}$ 4.38, total 100.83. This gives the empirical formula $\text{Na}_{1.88}\text{Mg}_{1.06}\text{Fe}_{0.01}^{2+}\text{P}_{1.00}\text{O}_{4.00}\text{F}_{1.00}$ based on 5 anions pfu. The strongest lines in the calculated X-ray powder-diffraction pattern [d_{calc} Å ($I_{\text{calc}}\%$)] are: 3.909 (75; 121), 3.382 (52; 023), 2.955 (90; 042), 2.606 (100; 200), 2.571 (96; 142), 2.545 (68; 104), 1.955 (83; 242), 1.691 (67; 046). Single-crystal X-ray diffraction data collected on a crystal of size $34\times 30\times 25\ \mu\text{m}$ refined to $R_1 = 0.019$ for 830 unique $I \geq 2\sigma(I)$ reflections shows moraskoite is orthorhombic, space group $Pbcn$ with $a = 5.2117(10)$, $b = 13.711(3)$, $c = 11.665(2)$ Å, $V = 833.6\ \text{Å}^3$, and $Z = 8$. The structure of moraskoite consists of $(\text{FNa}_4\text{Mg}_2)^{7+}$ octahedra that share faces to produce $[\text{FNa}_2\text{Mg}]^{3+}$ chains parallel to the a axis with phosphate ions located between them. Moraskoite is named after the host meteorite and Morasko village, near the location of the original discovery. Type material is deposited in the Mineralogical Museum of the University of Wrocław, Poland. **O.C.G.**

NICKELPICROMERITE*

E.V. Belogub, S.V. Krivovichev, I.V. Pekov, A.M. Kuznetsov, V.O. Yapaskurt, V.A. Kotlyarov, N.V. Chukanov and D.I. Belakovskiy (2015) Nickelpicromerite, $\text{K}_2\text{Ni}(\text{SO}_4)_2 \cdot 6\text{H}_2\text{O}$, a new picromerite-group mineral from Slyudorudnik, South Urals, Russia. *Mineralogy and Petrology*, 109, 143–152.

Nickelpicromerite (IMA 2012-053), ideally $\text{K}_2\text{Ni}(\text{SO}_4)_2 \cdot 6\text{H}_2\text{O}$, is a new supergene mineral found at the vein #169 of the Ufaley quartz deposit, near the town of Slyudorudnik, Kyshtym District, Chelyabinsk area, South Urals, Russia ($55^\circ 40' 12''\text{N}$ $60^\circ 21' 17''\text{E}$). It occurs with gypsum and goethite in fractures of slightly weathered actinolite-talc schist containing partially altered (vermiculitized) biotite, sulfides (pyrrhotite, pentlandite, millerite, pyrite, and marcasite) and, rarely, unaltered chromite. Nickelpicromerite occurs as equant to short prismatic or tabular crystals up to 0.07 mm and anhedral grains up to 0.5 mm (typically < 0.1 mm). The mineral is transparent, light greenish blue (light turquoise-colored), with white streak and vitreous luster. It does not fluoresce either in UV or in cathode rays. It is brittle with stepped fracture and Mohs hardness $\sim 2\text{--}2\frac{1}{2}$. $D_{\text{meas}} = 2.20(2)$ g/cm^3 (by flotation in $\text{CHBr}_3 + \text{CH}_3\text{OH}$); $D_{\text{calc}} = 2.222$ g/cm^3 . Nickelpicromerite is optically biaxial (+), with $\alpha = 1.486(2)$, $\beta = 1.489(2)$, $\gamma = 1.494(2)$ ($\lambda = 589$ nm); $2V_{\text{meas}} = 75(10)^\circ$, $2V_{\text{calc}} = 76^\circ$. FTIR spectra of nickelpicromerite and picromerite are very similar. Bands that could be assigned to NH_4^+ cations or CO_3^{2-} and NO_3^- anions in the range $1300\text{--}1500\ \text{cm}^{-1}$ are absent. O-H stretching vibrations are observed at $3237\ \text{cm}^{-1}$ (with three shoulders at 3365, 3290, and $3180\ \text{cm}^{-1}$) and weak H-O-H bending vibrations are observed at 1622 and $1560\ \text{cm}^{-1}$. Average of 5 electron probe WDS analyses (using rastered over $10\times 10\ \mu\text{m}^2$ beam) is [wt%

(range)]: K_2O 20.93 (20.0–22.1), MgO 0.38 (0–1.0), FeO 0.07 (0–0.2), NiO 16.76 (15.6–17.4), SO_3 37.20 (35.9–38.3), H_2O (calculated by difference) 24.66, total 100.00. The empirical formula, calculated on the basis of 14 O apfu is: $\text{K}_{1.93}\text{Mg}_{0.04}\text{Ni}_{0.98}\text{S}_{2.02}\text{O}_{8.05}(\text{H}_2\text{O})_{5.95}$. The strongest X-ray powder diffraction lines [d Å ($I\%$; hkl)] are: 5.386 (34; 110), 4.312 (46; 002); 4.240 (33; 120), 4.085 (100; 012, $10\bar{2}$), 3.685 (85; 031), 3.041 (45; 040, 112), 2.808 (31; 013, $20\bar{2}$, 122), 2.368 (34; $13\bar{3}$, $21\bar{3}$, 033). Unit-cell parameters calculated from the powder data are: $a = 6.13(1)$, $b = 12.22(1)$, $c = 8.98(2)$ Å, $\beta = 105.1(1)^\circ$, $V = 650\ \text{Å}^3$. Refinement of X-ray diffraction data collected on a single-crystal ($220\times 160\times 120\ \mu\text{m}$) yielded $R_1 = 0.028$ for 1585 unique $F > 4\sigma(F)$ reflections. Nickelpicromerite is monoclinic, $P2_1/c$, with unit-cell parameters of $a = 6.1310(7)$, $b = 12.1863(14)$, $c = 9.0076(10)$ Å, $\beta = 105.045(2)^\circ$, $V = 649.9\ \text{Å}^3$, $Z = 2$. Nickelpicromerite is isostructural to other picromerite-group minerals and synthetic Tutton's salts with the general formula $A_2M^{2+}(\text{SO}_4)_2 \cdot 6\text{H}_2\text{O}$. Its structure consist of $[\text{Ni}(\text{H}_2\text{O})_6]^{2+}$ octahedral cations linked to $(\text{SO}_4)^{2-}$ tetrahedra via complex system of hydrogen bonds, and K^+ cations coordinated by eight anions. The cotype specimens are deposited in the Natural Scientific Museum of the Ilmen State Reserve, Miass (catalogue number 17301), and in the Fersman Mineralogical Museum of the Russian Academy of Sciences, Moscow. **F.C.**

PILAWITE-(Ce)*

A. Pieczka, F.C. Hawthorne, M.A. Cooper, E. Szełęg, A. Szuszkiewicz, K. Turniak, K. Nejbert and S. Ilnicki (2015) Pilawite-(Y), $\text{Ca}_2(\text{Y,Yb})_2[\text{Al}_4(\text{SiO}_4)_4\text{O}_2(\text{OH})_2]$, a new mineral from the Piława Górna granitic pegmatite, southwestern Poland: mineralogical data, crystal structure and association. *Mineralogical Magazine*, 79(5), 1143–1157.

Pilawite-(Ce) (IMA 2013-125), with formula $\text{Ca}_2(\text{Y,Yb})_2[\text{Al}_4(\text{SiO}_4)_4\text{O}_2(\text{OH})_2]$, is a new mineral from a granitic pegmatite at Piława Górna in Lower Silesia, Poland ($50^\circ 42' 11.77''\text{N}$ $16^\circ 44' 12.36''\text{E}$). It occurs together with keiviite-(Y), gadolinite-(Y), hingganite-(Y), and hellandite-(Y), as inclusions in accessory allanite-(Y) within the blocky feldspar zone of a weakly zoned and weakly fractionated NYF affiliated dike, part of co-genetic pegmatites known as the Julianna pegmatitic system. The accessory minerals of the feldspar zone are black tourmaline, abundant zircon, monazite-(Ce), xenotime-(Y), single aggregates of allanite-group minerals and occasional Nb-Ta oxides (ixiolite with inclusions of cassiterite, fersmite, rutile, and ilmenorutile). Pilawite-(Y) occurs as an aggregate ~ 2 mm across, of 2–3 crystals reaching 1.5 mm long, enclosed in quartz and partly overgrown by allanite-(Y). Pilawite-(Ce) has white color and streak and a vitreous luster. Crystals are brittle and Mohs hardness is 5. Parting or cleavage are not observed. $D_{\text{calc}} = 4.007\ \text{g/cm}^3$. Pilawite-(Y) is non-pleochroic, optically biaxial (+), with $\alpha = 1.743(5)$, $\beta = 1.754(5)$, $\gamma = 1.779(5)$ (light not reported); $2V_{\text{meas}} = 65(2)^\circ$, $2V_{\text{calc}} = 68^\circ$, orientation $X \wedge a = 87.5^\circ$ (β acute), $Y // b$ and $Z \wedge a = 3.1^\circ$ (β obtuse). FTIR spectrum of pilawite-(Ce) shows broad prominent band at $\sim 2975\ \text{cm}^{-1}$, a sharp band at $\sim 2300\ \text{cm}^{-1}$ and a rather ragged weaker doublet centered at $\sim 2050\ \text{cm}^{-1}$, which can be related to O-H stretching modes. The Raman spectrum shows prominent Si-O stretching

bands in the range ~850–950 cm⁻¹ and a large number of Al–O modes and lattice modes below ~600 cm⁻¹. Average of 33 electron probe WDS spot analyses is [wt% (range)]: P₂O₅ 0.04 (0–0.30), SiO₂ 28.34 (28.16–28.68), TiO₂ 0.26 (0–0.82), Al₂O₃ 23.36 (22.61–23.87), Fe₂O₃ 0.72 (0–1.18), Y₂O₃ 22.17 (21.01–23.209), Gd₂O₃ 0.50 (0.18–0.80), Tb₂O₃ 0.21 (0.09–0.33), Dy₂O₃ 2.13 (1.35–2.83), Ho₂O₃ 0.54 (0.31–0.78), Er₂O₃ 2.04 (1.60–2.44), Tm₂O₃ 0.34 (0.17–0.47), Yb₂O₃ 2.53 (1.38–3.75), Lu₂O₃ 0.47 (0.30–0.75), FeO 0.32 (0–1.06), MnO 0.75 (0.59–1.34), CaO 12.50 (11.66–13.37), PbO 0.18 (0.12–0.28), H₂O (by stoichiometry and Fe³⁺/Fe²⁺ adjusted to maintain 12 cations pfu) 2.14 (2.11–2.16), total 99.55. The empirical formula, calculated on the basis of 20 O pfu is: (Ca_{1.88}Mn_{0.09}Fe_{0.04}Pb_{0.01})_{Σ2.02}(Y_{1.65}Yb_{0.11}Dy_{0.10}Er_{0.09}Gd_{0.02}Ho_{0.02}Tm_{0.02}Lu_{0.02}Tb_{0.01})_{Σ2.04}[(Al_{3.86}Fe_{0.08}Ti_{0.03})_{Σ3.97}(Si_{3.98}O₄)₄O₂(OH)₂]. The strongest X-ray powder diffraction lines [*d* Å (*F*%; *hkl*)] are: 3.921 (38; 112), 3.044 (100; 022), 2.791 (43; 004); 2.651 (46; 310), 2.583 (54; $\bar{3}11, 311$), 2.485 (62; $\bar{2}22, 114, 123$), 2.408 (45; $\bar{3}12$), 1.670 (36, 240). Refinement of X-ray diffraction data collected on a single crystal (40×40×50 μm) yielded *R*₁ = 0.0276 for 2009 unique *F* > 4σ(*F*) reflections. Pilawite-(Ce) is monoclinic, *P*2₁/*c*, with unit-cell parameters of *a* = 8.571(5), *b* = 7.261(4), *c* = 11.187(6) Å, β = 91.00(2)°, *V* = 696.1 Å³, *Z* = 2. Pilawite-(Ce) structure consists of chains of edge- and corner-sharing octahedra decorated by tetrahedra and having the stoichiometry [Al₂(SiO₄)₄O(OH)] that link by sharing corners to form an octahedron-tetrahedron framework with large interstices that contain Ca²⁺ and (Y,*Ln*)³⁺. Pilawite-(Ce) is a graphical isomer of the Al-P framework in palermoite, Sr₂Li₄[Al₂(PO₄)₂(OH)₂]₂. The name of the mineral is for the type locality, Pilawa Górna, in Lower Silesia, Poland. The holotype is preserved at the Mineralogical Museum of the University of Wrocław, Poland, in the form of one polished 1-inch disk with the catalogue number MMWr IV7676. **F.C.**

RALPHCANNONITE*

L. Bindi, C. Biagioni, T. Raber, P. Roth and F. Nestola (2015) Ralphcannonite, AgZn₂TlAs₂S₆, a new mineral of the routhierite isotypic series from Lengenbach, Binn Valley, Switzerland. *Mineralogical Magazine*, 79(5), 1089–1098.

The new member of the routhierite isotypic series, ralphcannonite (IMA 2014077), ideally AgZn₂TlAs₂S₆, was discovered in the specimen from massif sulfosalts accumulations in dolostone of the Lengenbach quarry, Binn Valley, Wallis, Switzerland. This well-known deposit is the type locality for 15 other thallium sulfosalts. Ralphcannonite is associated with dufrénoysite, hatchite, realgar, and barite. It forms black metallic euhedral equant crystals up to 50 μm with the prism {110} and pinacoid {001} as the dominant forms and bipyramids {101} and {111}, and prism {100} as an accessory forms. The mineral has black streak and is brittle with an irregular fracture. The micro-indentation hardness VHN₃₀ = 120 (116–128) kg/mm² corresponds to ~2–2½ of Mohs scale. The density was not measured; *D*_{calc} = 4.927 g/cm³. In plane-polarized incident light, ralphcannonite is grayish. Under crossed polars, it is very weakly anisotropic, with grayish to light blue rotation tints. Internal reflections are very weak. No optical evidence of growth zonation was observed. The reflectance values for COM wavelengths in air are: [*R*_{min},

*R*_{max}% (λ nm)]: 25.8, 27.1(471.1); 25.2, 26.6 (548.3); 24.6, 25.8 (586.6); 23.9, 24.8 (652.3). The average of electron probe WDS analyses (number not given) is [wt% (range)]: Cu 2.01 (1.78–2.22), Ag 8.50 (8.19–8.80), Zn 10.94 (10.25–11.33), Fe 3.25 (3.10–3.34), Hg 7.92 (7.10–8.50), Tl 24.58 (23.87–25.26), As 18.36 (17.58–18.96), Sb 0.17 (0.09–0.25), S 24.03 (23.61–24.66), total 99.76. Other elements with *Z* > 9 were not detected. The empirical formula based on 12 atoms pfu is (Ag_{0.63}Cu_{0.25}Zn_{1.35})Fe_{0.47}Hg_{0.32}Tl_{0.97}(As_{1.97}Sb_{0.01})_{Σ1.98}S_{6.03}. Due to the very small size and amount of crystals available, a powder X-ray diffraction pattern was not collected. The strongest lines of the calculated X-ray powder diffraction pattern [*d*_{calc} Å (*I*_{calc}%; *hkl*)] are: 4.100 (85; 211), 3.471 (40; 103), 2.954 (100; 222), 2.656 (20; 321), 2.465 (400), 2.460 (39; 303). The crystal structure has been solved on the basis of the X-ray single-crystal data and refined to *R*₁ = 0.030 for 140 observed [*F*_o > 4σ(*F*_o)] reflections. The mineral is tetragonal, $\bar{4}2m$, with *a* = 9.861(2), *c* = 11.125(3) Å, *V* = 1081.8 Å³, *Z* = 4. The crystal structure of ralphcannonite is isotypic with those of routhierite, staldelite and arsiccioite showing a framework of corner sharing (Ag,Zn) S₄ tetrahedra (1 M1 + 2 M2), with channels along [001] hosting TlS₆ orthorhombic pyramids and (As,Sb)S₃ dissymmetric trigonal pyramids sharing corners and edges with the tetrahedron framework. Ralphcannonite is derived from routhierite M¹Cu^{M2}Hg₂TlAs₂S₆ through the double heterovalent substitution M¹Cu⁺ + M²Hg²⁺ → M¹Zn²⁺ + M²Ag⁺. This substitution obeys a steric constraint, with Ag⁺, the largest cation relative to Zn²⁺ and Cu⁺, occupying the largest M2 site, as observed in arsiccioite. The ideal crystal-chemical formula of ralphcannonite is M¹Zn^{M2}(Zn_{0.5}Ag_{0.5})₂TlAs₂S₆. The name honors Ralph Cannon (b. 1956) for his contribution to the knowledge of the mineralogy of the Lengenbach quarry. The holotype specimen of ralphcannonite is deposited in the Museo di Storia Naturale, Università degli Studi di Firenze, Florence, Italy. **D.B.**

YEOMANITE*

R.W. Turner, O.I. Siidra, M.S. Rumsey, Y.S. Polekhovskiy, Y.L. Kretser, S.V. Krivovichev, J. Spratt and C.J. Stanley (2015) Yeomanite, Pb₂O(OH)Cl, a new chain-structured Pb oxychloride from Merehead Quarry, Somerset, England. *Mineralogical Magazine*, 79(5), 1203–1211.

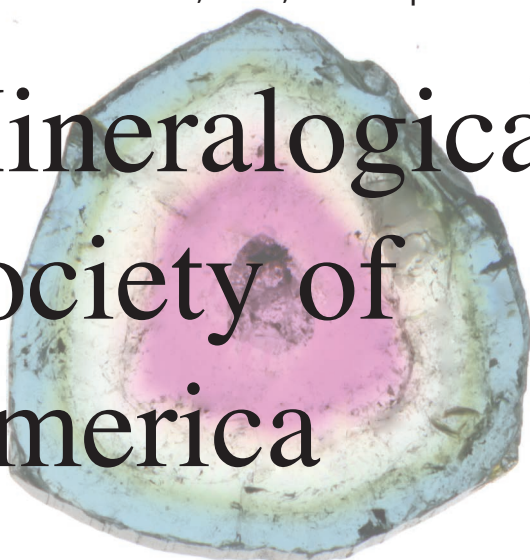
Yeomanite (IMA 2013-024), ideally Pb₂O(OH)Cl, is a new mineral found in the Mn pod mineral assemblage at Merehead (Torr Works) Quarry, near Cranmore, Somerset, England. The new mineral is named after Angela Yeoman (b. 1931) and her company, Foster Yeoman, which had been operated at the Quarry until 2006. The new mineral was found in cavities in manganese oxide pods (a mixture of manganite and pyrolusite, associated with goethite, and gangue minerals such as aragonite, calcite, and barite) that have thin rims of calcite lining the outermost edges. These cavities are filled by either mendipite, Pb₃Cl₂O₂, or by asbestos-like fibrous aggregates of yeomanite. Other oxychloride minerals found in those pods include chloroxiphite, diabolite, mereheadite, paralaurionite, parkinsonite, symesite, rickturnerite, and rumseyite. Mimetite, wulfenite, cerussite, “hydrocerussite,” malachite, and “crednerite” occur in the same environment. Yeomanite fibers (up to 15 mm, generally <8 mm long) form

loose mats and strands, and individual fibers are. Yeomanite is white, occasionally pale gray, transparent, with a white streak and a vitreous luster. It does not fluoresce in UV radiation. The mineral is brittle. The micro-indentation hardness $VHN_{20} = 54.5$ kg/mm² corresponding to ~2 of the Mohs scale. The perfect cleavage is parallel to fibers elongation. Density was not measured due to the fibrous nature; $D_{\text{calc}} = 7.303$ g/cm³. In reflected light, yeomanite is light gray to gray with white internal reflections, non-pleochroic and does not have birefractance. The reflectance values in air [R_{min} , R_{max} (nm)] are: 16.0, 20.2 (400), 15.4, 19.5 (420), 15.0, 18.9 (440), 14.7, 18.6 (460), 14.5, 18.4 (470), 14.4, 18.2 (480), 14.1, 17.8 (500), 13.9, 17.5 (520), 13.7, 17.3 (540), 13.7, 17.2 (546), 13.5, 17.1 (560), 13.3, 16.9 (580), 13.3, 16.8 (589), 13.2, 16.8 (600), 13.1, 16.7 (620), 13.0, 16.6 (640), 12.9, 16.6 (650), 12.8, 16.6 (660), 12.8, 16.5 (680), 12.8, 16.4 (700). The anisotropism $\Delta R_{589} = 3.58\%$. The average of 20 electron

probe EDS analyses on three crystals of yeomanite is [(wt%, (range)): PbO 92.3 (91.97–92.50), Cl 7.4 (7.35–7.48), H₂O 1.9 (by structure data), O=Cl 1.7, total 99.9. The formula calculated on the basis of 3 O+OH+Cl pfu is: $Pb_{1.99}O_{0.98}(OH)_{1.01}Cl_{1.01}$. The strongest lines of the X-ray powder diffraction pattern [d Å (hkl)] are: 2.880 (100; 113), 2.802 (78; 006), 3.293 (61; 200), 3.770 (32; 011), 2.166 (22; 206), 1.662 (19; 119), 2.050 (18; 303), 3.054 (17; 105). The crystal structure of yeomanite was solved by direct methods and refined to $R_1 = 10.6\%$. The mineral is orthorhombic, $Pnma$, $a = 6.585(10)$, $b = 3.855(6)$, $c = 17.26(1)$ Å, $V = 438$ Å³, and $Z = 4$. Crystal structure of yeomanite is based on $[O(OH)Pb_2]^+$ chains that are formed by oxycentered OPb_4 tetrahedra joined by $OHPb_3$ triangles. The holotype specimen is housed in the Natural History Museum, London, England, and a cotype specimen is stored in the Smithsonian Institution in Washington, D.C., U.S.A. **Yu.U.**

Interested in minerals, rocks, and the processes that form them? Learn about the

Mineralogical Society of America



www.minsocam.org

Mineralogical Society of America 3635 Concorde Pkwy Ste 500 Chantilly VA 20151-1110 USA
phone: +1 (703) 652-9950 fax: +1 (703) 652-9951

(Sliced and polished, color-zones tourmaline, Plumbago Mining's Newry or Mt. Mica deposit, Newry, Maine, U.S.A.)

Awards
Short Courses
Specialist Groups
Collector's Corner
Mineralogy 4 Kids
Member Discounts
Ask-a-Mineralogist
MSA-Talk list-serve
Elements – magazine
Lectureship Program
Student Research Grants
Monographs and Textbooks
Symposia and Special Sessions
American Mineralogist - journal
Reviews in Mineralogy and Geochemistry

